PV Maximum Power Point Tracking Through Pyranometric Sensor: Modelling and Characterization

A.Lay-Ekuakille[1], G. Vendramin[1], A. Fedele[1], L. Vasanelli[1], A. Trotta [2]

[1]Dipartimento d'Ingegneria dell'Innovazione, University of Salento

Via Monteroni, 73100 Lecce, Italy, aime.lay.ekuakille@unile.it http://smaasis-misure.unile.it

[2]Dipartimento di Elettrotecnica ed Elettronica, Polytechnic of Bari, Via Orabona, 70100 Bari, Italy

Abstract – Solar trackers represent apparatuses that may significantly improve electric power production of photovoltaic panels. For detecting solar position, the trackers use different sensors (e.g. photoresistor, photodiode receiver, phototransistor, etc..). This research proposes an alternative way, the use of the sensor par excellence for retrieving solar radiation; the pyranometer. A design and tests have been performed in order to show the improvements. A comparison has been made between this alternative mounted on a solar follower plant and another tracking system called S.A.I.S. which does not use any solar position sensor but tracks the panel by solar position calculations, from the ad hoc knowledge of longitude, latitude, date and hour. A second comparison has been also made between the above pyranometer architecture and a specifically designed solarimeter.

Index terms*:* PV system, MPPT, pyranometer, modelling, solar irradiance, solar tracker, solarimeter.

I. INTRODUCTION

The idea of using a pyranometer as sensor for the detection of solar position is related to two special needs:

- first of all, it is the most suitable instrument for the measurement of solar radiation since this parameter is more important than sun position;
- secondly, one should not forget that, in conditions of cloudy sky, there could be a small component of direct radiation and a substantial component of diffuse radiation [1-4]. Using a pyranometer the PV (photovoltaic panel) can be located in order to be able to absorb the greatest amount of radiation as possible.

Since the phenomenon of cloudy sky is uncertain, one could find in the situation in which the most radiation is obtained by providing the panel in a manner not perpendicular to sunlight, in the cases in which, for example, the sky is cloudy and the diffused component is more greater

towards different directions to the "panel-sun" one [5]. Among all the variables affecting the Earth radiation budget there is one of particular importance: the total broadband solar irradiance incident at the surface of the Earth. This is the amount of radiant energy coming from the sun that is not absorbed nor back-scattered by the atmosphere and hence reaches the surface of the Earth. The total broadband solar irradiance is important in atmospheric sciences because it is intimately related to the understanding of atmospheric composition, gaseous absorption, molecular and particular scattering and radiative transfer theory. All of these elements provide valuable information to understand the Earth radiation budget and therefore to understand climate, as well. Ground measurements of the total broadband solar radiation can be done in two different ways: directly or using the so-called component summation technique. The first technique consists of using a radiometer called pyranometer, which is the primary object of study of the present research. Pyranometers were first designed to measure total broadband solar radiation incident on the surface of the Earth. The pyranometer output presents, however, a dependence on the angle of incidence of the incoming radiation. This dependence, called cosine error, can produce a significant error in the measurement. Manufacturers try to minimize the cosine error in the instrument design and in the calibration procedure of the instruments. Although it can be minimized, the cosine error cannot be eliminated completely from the measurement [6].

Pyranometers dedicated for solar energy measurements fall into one of two main categories: those that measure the temperature rise of a black surface referenced against a thermal mass or a reflective white surface, and those that convert radiant energy directly to electrical energy, that is, photometric types. The black surface pyranometers typically offer spectrally uniform response from 300 to 3000 nm and some meet or exceed the WMO (World Meteorological Organization) specifications suggested for high quality instruments suitable for use as secondary standard measurements [7].

This paper is organized as follows: section II deals with solar radiation computation that is necessary to understand the operating mode of fixed and tracking PV plants. The facility used to perform the experiments is described in section III, while the design of the electronic board capable of performing the control of S.A.I.S. plant and a simulation code of retrieving sun trajectory are illustrated in section IV. An empirical assessment of the model, using a linear actuator and rotative motor is depicted in section V. Results are presented in section VI by taking into account a designed solarimeter.

II. SOLAR RADIATION COMPUTATION

The problem of the evaluation of incident solar radiation on a surface can only be tackled with cautious approximation because of many variables are involved and their unpredictability (presence of clouds, atmosphere transparency, etc.). The solar radiation incidence depends on two fundamental parameters: *height of the sun* and *its position*. Figure 1 shows the position of the sun along its apparent trajectory during the identified day by two angles:

- β: *solar elevation*, angle provided by the right that joins respectively the centres of the earth and the sun with the horizontal plane;
- Ψ: *Azimuth angle*, formed by the projection of sun-earth right on horizontal plane with the North-South direction.

Once the angles are known, it is possible to determine the instantaneous solar position, in order to assess the energy flow of incident solar radiation on a surface that allows the determination of the *incidence angle* (figure 2) between the normal to the surface and the solar rays (sun-surface right).

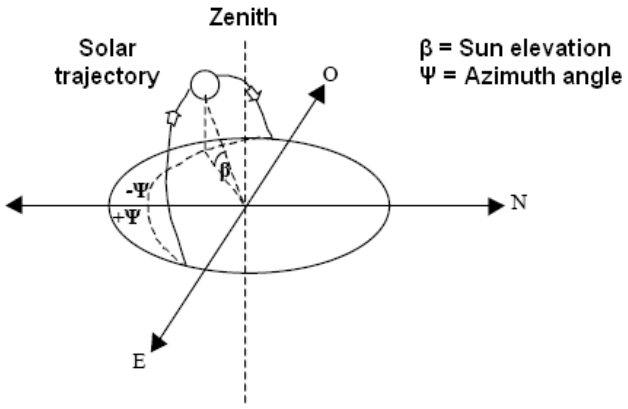

Figure 1. Solar position.

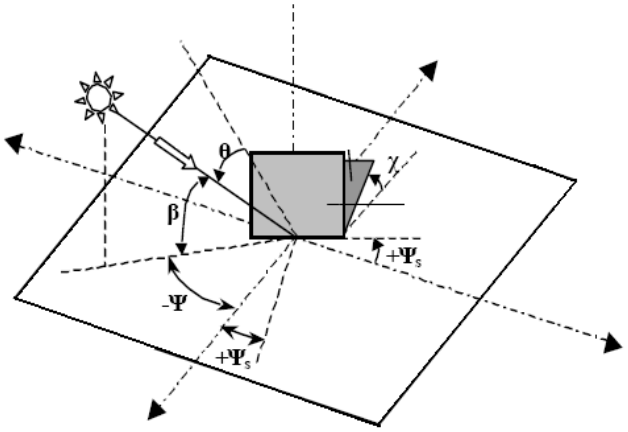

Figure 2. Solar position with surfaces of different inclination and orientation.

It is therefore necessary, to know:

- χ: *surface inclination*, angle between the surface and the horizontal plane;
- Ψs: *Azimuth of surface*, angle measured on the horizontal plane between the normal to the surface and the North-South direction.

Since the following equation is valid:

$$\cos\theta = \cos\beta \cdot \cos(\Psi - \Psi_S) \cdot \sin\chi + \sin\beta \cdot \cos\chi \qquad \text{(Valid for } \cos\theta > 0\text{)} \quad (1)$$

to assess the global solar flow on a surface of generic disposition and orientation in any sunny day (sum of solar radiation direct, diffuse and reflected from the ground), it must be necessary to refer to a model semi-empiric of "atmosphere" that allows a satisfactory degree of accuracy. The most used mathematical model is the one adopted by ASHRAE, which is based on the calculation of normal and diffuse radiation through appropriate relations. First of all, it is suitable to define the Solar constant φ_C as the *incident solar energy flow* per unit area on perpendicular surface to earth-sun right, out of the atmospheric layers and measured when the solar distance takes the average value. It results: $\varphi_C = 1353[W/m^2]$. Because of the orbit eccentricity, the distance earth-sun varies during a year and therefore the extra-atmospheric radiation φ_N varies according to the law:

$$\varphi_N = \varphi_C[1 + 0.033 \cdot \cos(360 \cdot g / 365)] \qquad (2)$$

where g represents the day of the year considered, counted from january 1. For example, the day february 3 corresponds to $g = 34$ (31+3). Therefore the radiation φ_T that reaches a surface (figure 3), in clear sky conditions, can be calculated as:

$$\varphi_T = \varphi_{dir} + \varphi_{diff} + \varphi_{refl} \qquad (3)$$

The direct component φ_{dir} on a surface is provided by:

$$\varphi_{dir} = \frac{A}{e^{\frac{B}{\sin\beta}}} \cdot \cos\theta \qquad \text{(Valid for } \cos\theta > 0\text{)} \quad (4)$$

where:

- A is the *extra-atmospheric radiation* that it would be if the origin of the rays had zenithal. It is assessed for each day of the year by the formula:

$$A = 1150.65 + 72.43 \cdot \cos(0.95 \cdot g) + 34.25 \cdot \sin(0.017 \cdot g) + 1.5 \cdot \log(g) \quad (5)$$

- B is the *endangered atmosphere coefficient*. It is:

$$B = 1/(6.74 + 0.026 \cdot g - 5.13\,10^{-4} \cdot g^2 + 2.24.10^{-6} \cdot g^3 - 2.80 \cdot 10^{-9} \cdot g^4) \quad (6)$$

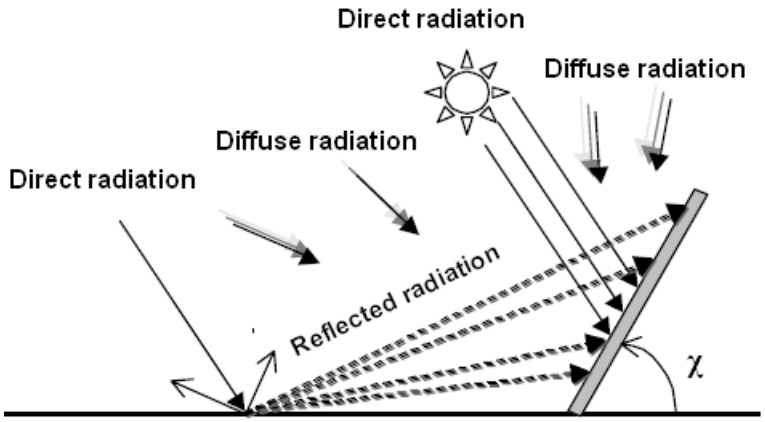

Figure 3. Global radiation on an inclined plan.

The *diffuse component* φ_{dir} on the same area is:

$$\varphi_{diff} = C \cdot \frac{A}{e^{\frac{B}{\sin\beta}}} \cdot F \quad (7)$$

where:

- *C* is the *diffuse radiation factor* calculable through:

$$C = 1/(16.9 + 0.0001 \cdot g - 8.65 \cdot 10^{-4} \cdot g^2 + 3.93 \cdot 10^{-6} \cdot g^3 - 4.005 \cdot 10^{-9} \cdot g^4) \quad (8)$$

- *F* is the *factor of view* between the considered surface and the sky:

$$F = \frac{1 + \cos\chi}{2} \quad (8)$$

If the surface is inclined, it receives less diffuse radiation from atmosphere, but it can receive an additional amount of reflected radiation φ_{refl} due to the reflection from the ground. The reflection factor is called **albedo**. It varies considerably depending on the nature of the soil, vegetation, etc. The component reflected may be determined as:

$$\varphi_{refl} = \frac{A}{e^{\frac{B}{\sin\beta}}} \cdot (C + \sin\beta) \cdot \rho_g \cdot (1 - F) \quad (9)$$

where ρ_g is the *reflection factor* of the surrounding ground (**albedo**).

III. FACILITY DESCRIPTION

A description of the facility with which experiments have been carried out; it included a mechanical system and a tracking algorithm. As regards this particular stage (mechanic part

and motors) it was used a Software for mechanic design (solidwoks), using a photovoltaic panel (780 x 490 x 33 mm) as depicted in figure 4. The structure of figure 5 has been used with the evidence of the two motors and its dimensions are expressed in millimetres.

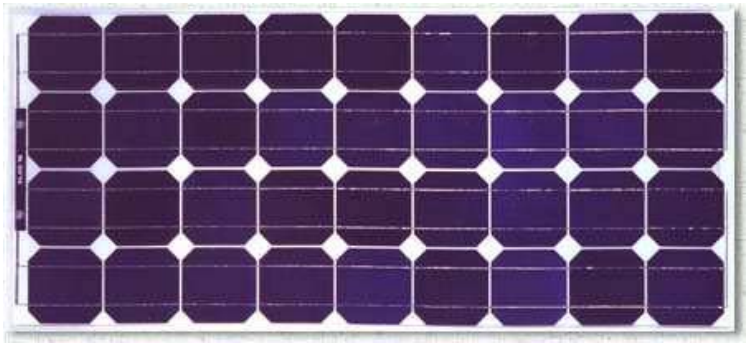

Figure 4. The monocrystalline panel BP solar.

Figure 6 shows the electronic connection with the PIC microcontroller used to supervise the structure dedicated to the experiment. As regards tracking algorithm, an "inspection method" of work area of automatic system has been performed according to the flowchart illustrated if figure 7; as matter of fact, the value of the radiation read by the pyranometer in a configuration is always compared with the value of previous configuration.

Figure 5. The Solidworks project and the used motors.

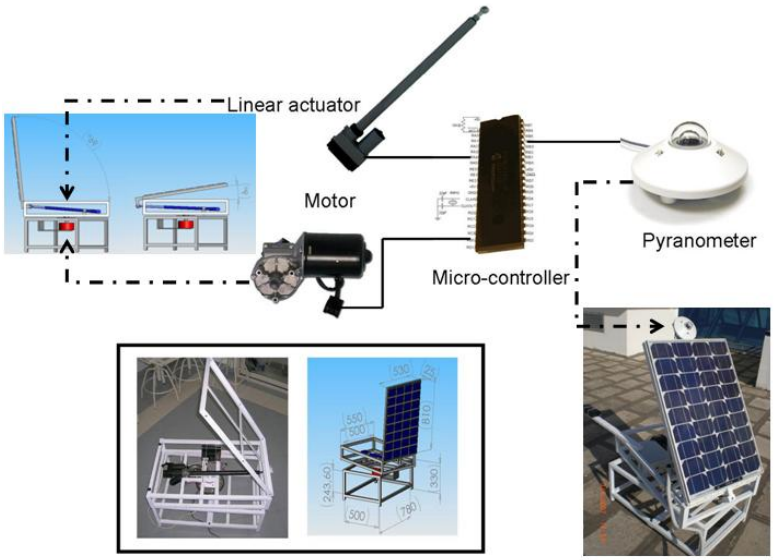

Figure 6. Architectural scheme.

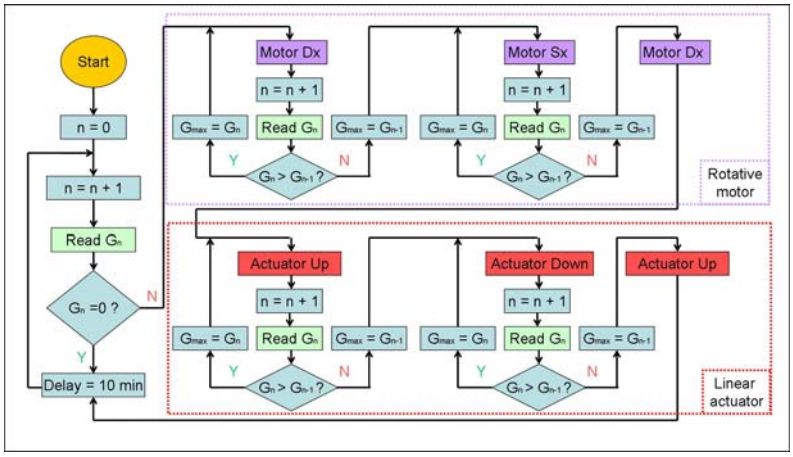

Figure 7. Flow chart.

As depicted the previous flowchart, the tracking takes place initially on the azimuth position, by means of the rotary motor and then on the zenithal position using a linear actuator. The tracking occurs every 10 minutes (delay) and the system is on stand-by configuration when the pyranometer does not find a value of radiation, when there is not sun in the sky.

IV. SIMULATIONS AND ELECTRONIC CIRCUIT BOARD

The main scope of simulations is predict the sun path for the envisaged PV system. For performing simulations, it was essential to implement a software that was able to compute the solar path diagram during the variation of the two fundamental geographical coordinates that are latitude and longitude, and to release the value of absorbed radiation by the panel either in

fixed configuration or in S. T. P. tracker. Thanks to this tool it is possible to know the apparent path followed by the sun in the sky for a period of about 25 years; that is the average life of photovoltaic panels. The tool is equipped with a graphical user interface through which the user is able to know the apparent path that the sun would follow in the sky in a given day of the year. Once started the tool, the user inserts latitude and longitude of the location for which he wishes to know the solar path. At this point [8], the user chooses the date (year, month and day) during which it is possible to see the solar path and, he starts the simulation. One will notice that, at this point, the sun [9], dynamically, describes the path [10] of the chosen day, as illustrated in figure 8, as, for example, the screen will appear in the day 08-01-2008.

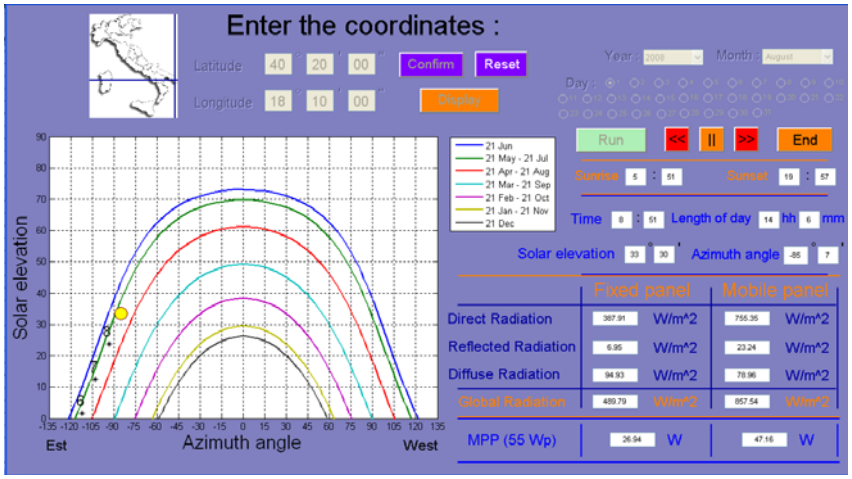

Figure 8. MATLAB simulation.

During the simulations the following items [11] are shown:

- The local time in which the sun rises and sets, or, more precisely, the hours during which the sun is situated in the horizon with a solar height equals to 0°;
- The duration of the day, obtained as difference between the two amounts introduced in the previous step.
- The local time.
- Solar elevation and azimuth angle.

As evidenced by figure 8 for a fixed panel and a mobile one, the values of global radiation, its components (direct, diffuse and reflected) and the value MPP (Maximum Power Point) for the panel are reported [12-16].

	Fixed panel		Mobile panel	
Direct Radiation	387.91	W/m^2	755.35	W/m^2
Reflected Radiation	6.95	W/m^2	23.24	W/m^2
Diffuse Radiation	94.93	W/m^2	78.96	W/m^2
Global Radiation	489.79	W/m^2	857.54	W/m^2
MPP (55 Wp)	26.94	W	47.16	W

Figure 9. Radiation and MPP for fixed and mobile panels.

Obviously, the simulations were performed during a sunny day in order to have elements without waiting the presence and concentration of clouds. An interesting fact is that the diffuse radiation of fixed panel is greater than the one of a mobile panel that follows the apparent path of the sun. That means there are some configurations, for example in the case of many clouds, in which the optimal layout of panels is not perpendicular [17] to sunlight. In this case, the global radiation will be represented by diffuse radiation, by taking [18] into account the shortage of direct radiation [19]. Here are, illustrated in figure 10 and figure 11, the results of simulations for the calculation of absorbed radiation by fixed panel [20-21], located towards the south with an elevation angle of 30° and the mobile panel in the city of Lecce (Latitude = 40° 20’ and Longitude = 18° 10’) in the day of Summer Solstice (June 21). Two devices (figure 12) were necessary for the simulations: MPPT 3000 and the pyranometer CM11.

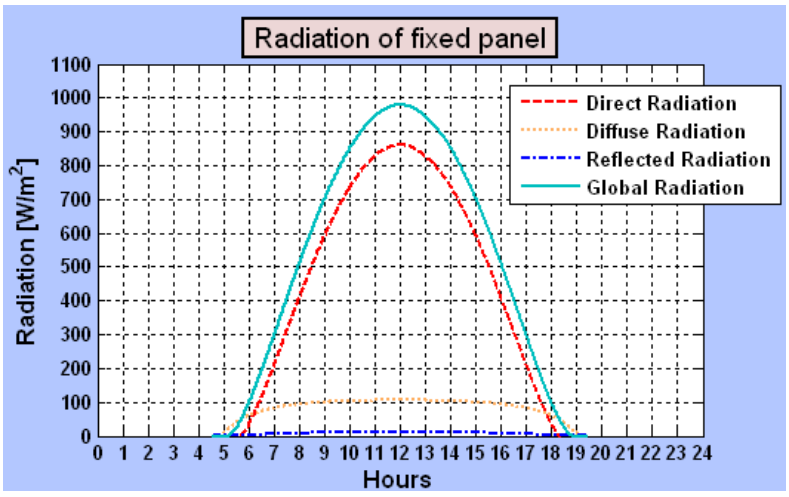

Figure 10. Radiation of Fixed panel (Lecce (Italy), 2008 June 21).

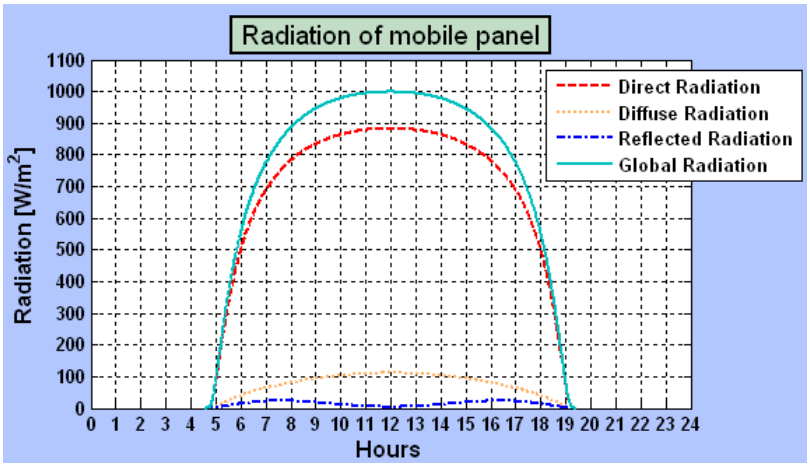

Figure 11. Radiation of Mobile panel (Lecce (Italy), 2008 June 21).

Figure 12. MPTT 3000 and CM11.

The Electronic circuit board, designed and built is shown in figure 13. It contains some important devices, namely, the PIC, the oscillators (Osc 1 and Osc 2).

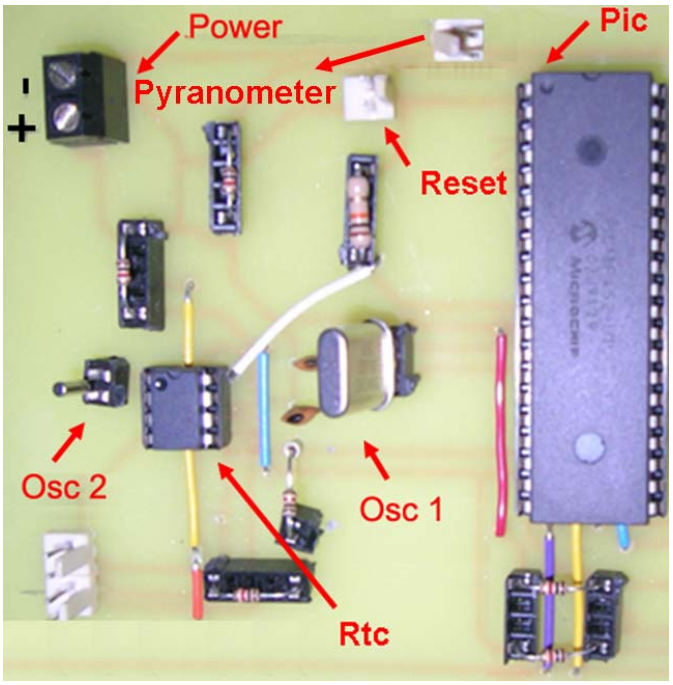

Figure 13. Electronic circuit board.

V. EMPIRICAL ESTIMATE OF THE MODEL

Since the microcontroller (PIC) provides a step, from 0V to 5V, to the driver of the motors during all times [22] that it enables the supervision; through the digital scope TDS 2024B, some measurements have been carried out in terms of characterization of the transient response (t_d, t_r, t_s) on each motor which will receive an input, through the driver, a step of size equals to 12V. In this way it is possible to characterize the system by identifying the two motors: rotary motor and linear actuator.For linear actuator the following parameters are obtained and illustrated in figures 14 and 15:

• delay time $t_d = 80ns = 80 \cdot 10^{-9} s$

• rise time $t_r = 162.6ns = 162.6 \cdot 10^{-9} s$

• settling time $t_s = 1\mu s = 1 \cdot 10^{-6} s$

By using the previous retrieved parameters, the following values for the *damping factor* and *natural pulsation* are yielded:

$$\zeta \approx 0.2 \qquad \omega_n \approx 1.5 \cdot 10^7 \quad (11)$$

Then the transfer function will be:

$$F_{att}(s) = \frac{2.25 \cdot 10^{14}}{s^2 + 0.6 \cdot 10^7 s + 2.25 \cdot 10^{14}} \quad (12)$$

with poles assuming:

$$p_1 = -0.3 \cdot 10^7 + 1.4697 \cdot 10^7 i \qquad p_2 = -0.3 \cdot 10^7 - 1.4697 \cdot 10^7 i$$

For the rotary motor**,** the following parameters are obtained and shown in figures 16 and 17 :

• delay time $t_d = 30\mu s = 30 \cdot 10^{-6} s$

• rise time $t_r = 38.28\mu s = 38.28 \cdot 10^{-6} s$

• settling time $t_s = 60\mu s = 60 \cdot 10^{-6} s$

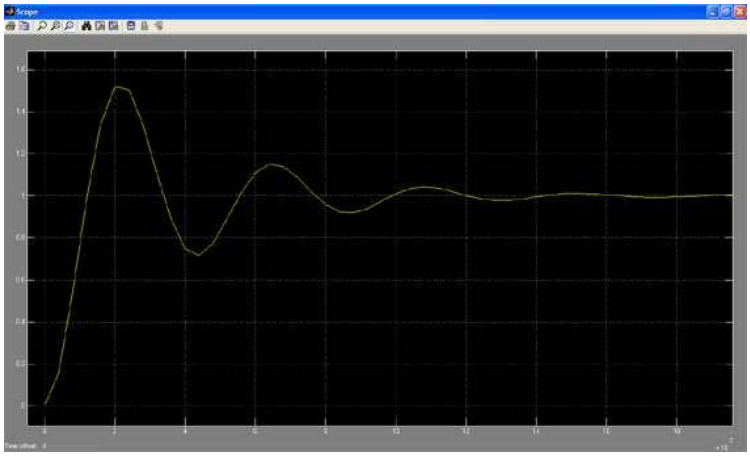

Figure 14. Output of linear actuator.

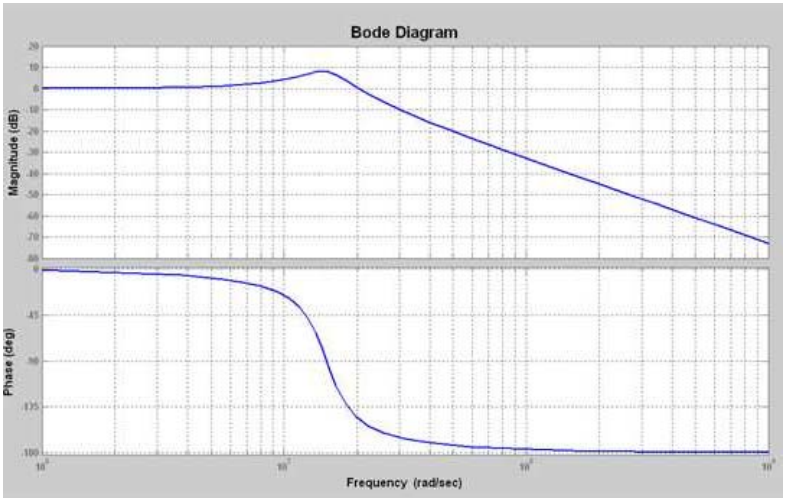

Figure 15. Bode diagram of linear actuator.

From which:

$$\zeta \approx 0.91 \qquad \omega_n \approx 5.5 \cdot 10^4 \quad (13)$$

The transfer function will then be:

$$F_{att}(s) = \frac{3 \cdot 10^9}{s^2 + 5.005 \cdot 10^4 s + 3 \cdot 10^9} \quad (14)$$

with poles equal to:

$$p_1 = -5.005 \cdot 10^4 + 2.2249 \cdot 10^4 i \qquad p_2 = -5.005 \cdot 10^4 - 2.2249 \cdot 10^4 i$$

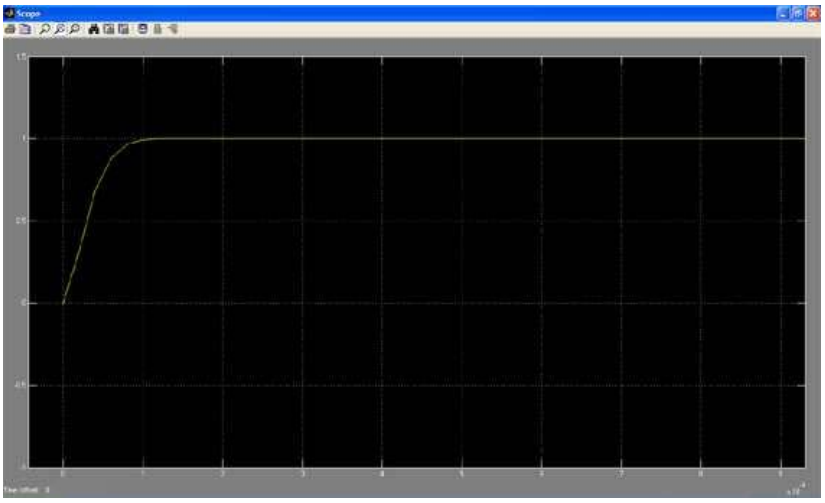

Figure 16. Output of rotational motor.

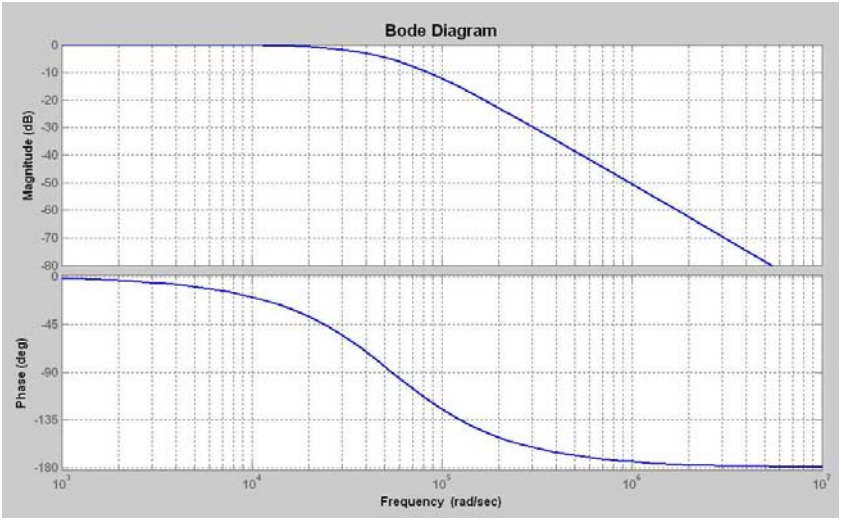

Figure 17. Bode diagram of rotational motor.

VI. RESULTS AND FINAL COMMENTS

The main aspects of this section concern the presentation of results by comparing the designed system called S.T.P. with a fixed one, in conditions of optimal configuration in Lecce city latitudes, that is, elevation of the panel at 30° and towards south; positive and interesting results are obtained. A first comparison regards the global radiation that hits the panel as shown in figure 18. Compared to fixed system, there is an increase of radiation of 38.7% even if the calculations were carried out for a sunny day.

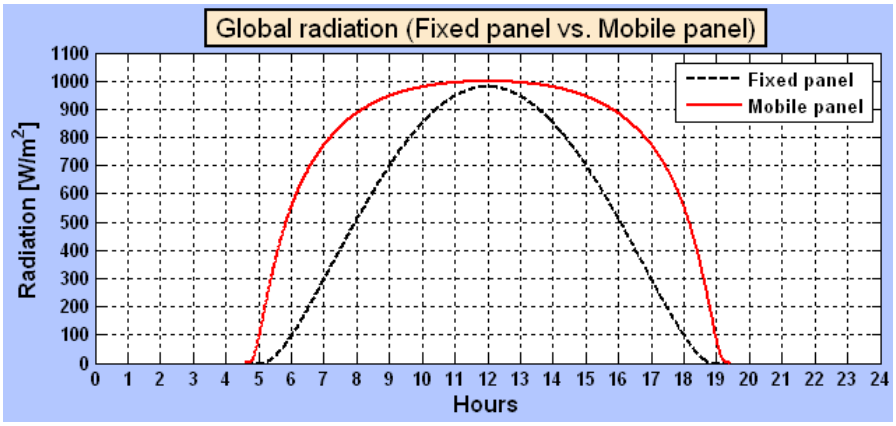

Figure 18. Global radiation (Fixed panel vs. S.T.P.).

By extrapolating the relationship between radiation and power of the photovoltaic panel, at the point of maximum power, through the use of the I-V characteristic, according to the radiation, a linear expression has been obtained. This means that, as expected, at an ideal temperature of 25°C, the power grows with the increasing radiation. On figure 19 it is evident to find the comparison between maximum power of the fixed system and maximum power with S.T.P. A further comparison, of great utility, has been made between S.T.P. and S.A.I.S. The difference, on field, between the two types of tracker is fundamental. The S.T.P. uses the pyranometer as sensor of solar radiation detection and makes the tracking thanks to algorithm described above. The S.A.I.S. does not use any sensor because it recognizes the position of the sun without seeing it. It automatically calculates the position of the sun and allows the panel to be oriented towards the correct and useful position. The latter suffers from a disadvantage: it is very important the "exact" positioning of the system, because also, a small deviation from ideal position could cause a considerable drop in terms of output power. All that does not occur with S.T.P., because it does not require an initial tuning.

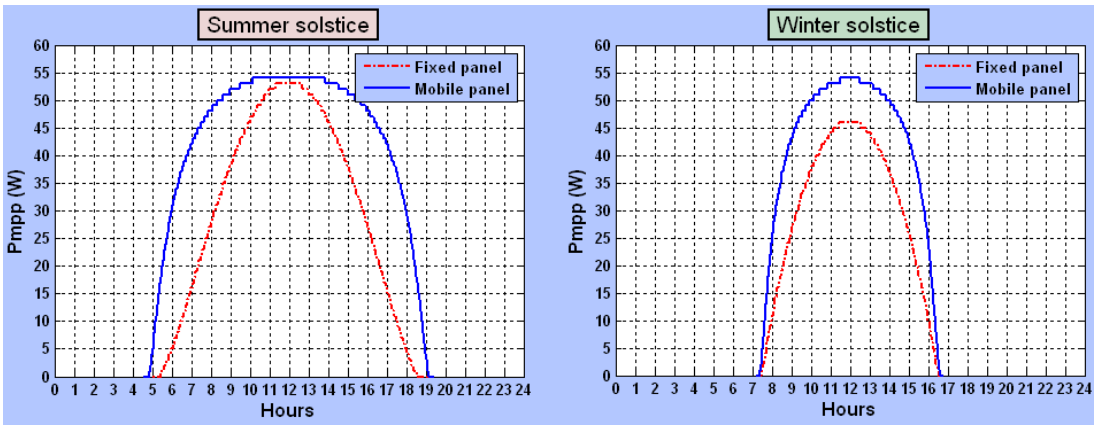

Figure 19. P_{mpp} (Fixed panel vs. S.T.P.).

Table 1 summarizes comparative data between fixed system, tracking with S.A.I.S. and tracking with S.T.P. for the panel of 55 W_p. In the calculation of performance, a simulated uniform distribution of clouds has been carried out that completely covers the sun for the 30% of the day.

Table 1: Comparison between different configurations of PV generators

	Fixed system	**S.A.I.S**	**S.T.P.**
Cost of the structure (with motors)	30 €	350 €	**350 €**
Cost of electronic components	0 €	100 €	**50 €**
Cost of the sensors	0 €	0 €	**600 €**
Total Cost	30 €	450 €	**1000 €**
Performance	16 %	21.28 %	**22.2 %**
Average radiation	456.98 W/m^2	481.12 W/m^2	**497.5 W/m^2**
Average power (55 W_p)	34.8 W	36.9 W	**38.1 W**

In short, a significant increase of output power of panel with tracker S.T.P. has been obtained. However, it is clear that the cost of a similar structure is unsustainable for small PV plants, for example 5 kW_p because it is prohibitive. It would be desirable to apply the pyranometer sensor to big plants. In future these results, simulated for now, will be tested on a real system that it is in progress. Beside the above study, a further sensing system capable of measuring sun radiation, it would be possible to use a small PV cell of 4 cm^2 as a sensor instead of a pyranometer as indicated in figure 20. This solarimeter board has been designed for the purposes of this research. It has four different sections, namely, from left to right, a reference voltage regulator with LM component, a DAC control circuit, a current amplifier circuit and a PGA (Programmable Gain Amplifier) block.

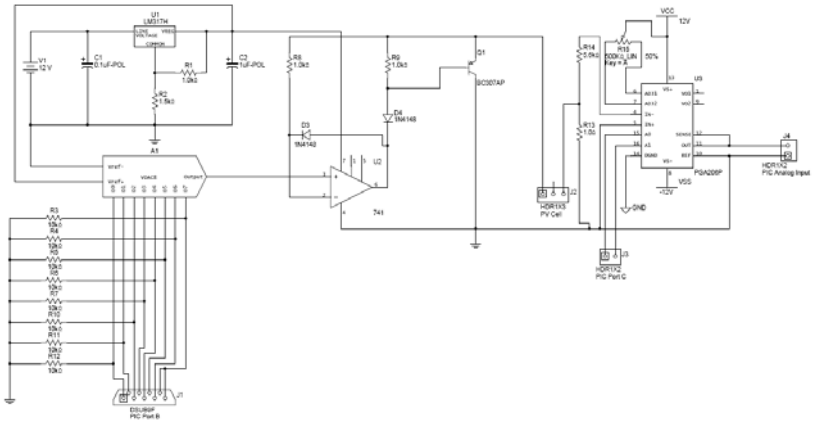

Figure 20. Solarimeter.

Once designed the solarimeter, some simulations have been performed in order to determine the current produced at specific irradiance of 1000 W/m^2 at 25°C: the current is 40 mA. In Standard Test Conditions (STC), the current density characteristic, as function of cell voltage, is illustrated in figure 21.

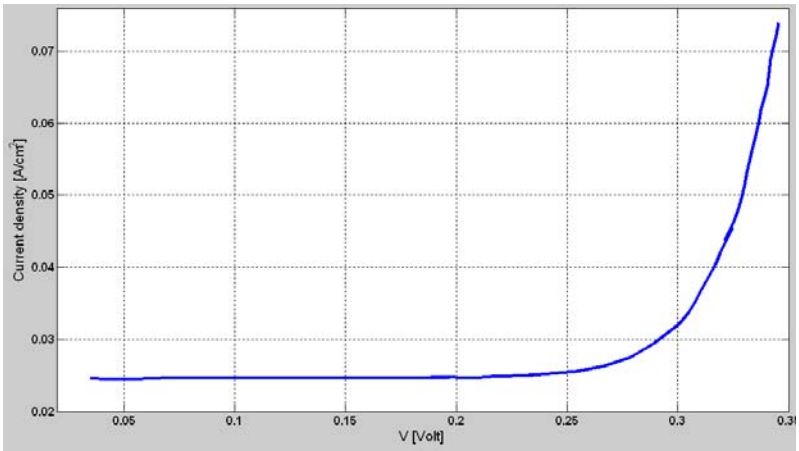

Figure 21. Current density characteristic.

Instead, in figure 22, the read point is the unique point does not vary with respect to temperature variation (0.23 V, 39.12 mA). To determine the load resistance and the reference voltage, it is necessary to vary the level of incident radiation on the cell at different values of temperature. A first measurement has been carried out at 35°C, by setting a halogen lamp at a power of 50 W and by varying the mobile cursor of a potentiometer, from the minimum up to the maximum value, by performing a punctual scanning. This operation has been repeated by setting the lamp at a power of 25 W. The second set of measurements has been carried out by decreasing the temperature up to 20°C. Consequently, the plot of figure 23 is obtained.

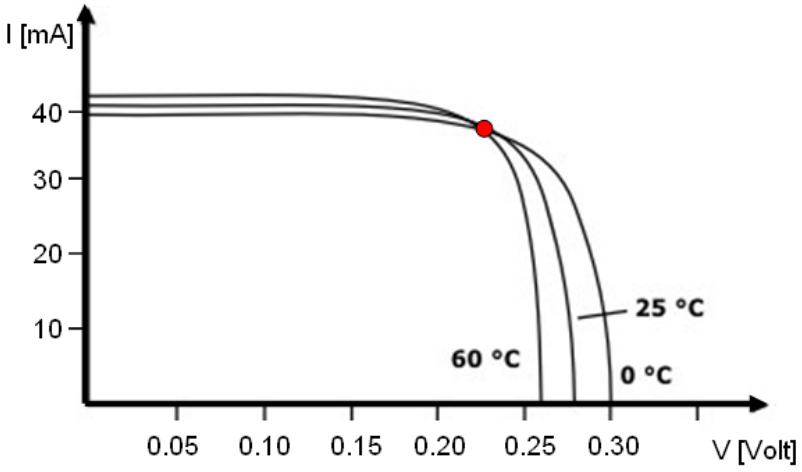

Figure 22. I-V characteristic.

The same plot illustrates the points of constant temperatures that have been interpolated by using the following equation:

$$I = 200\,V - 12 \qquad (15)$$

The value that the reference voltage must assume can be deduced from the intersection of the right with the voltage axe, so:

$$V_{ref} = 12 / 200 = 0.06\,V \quad (16)$$

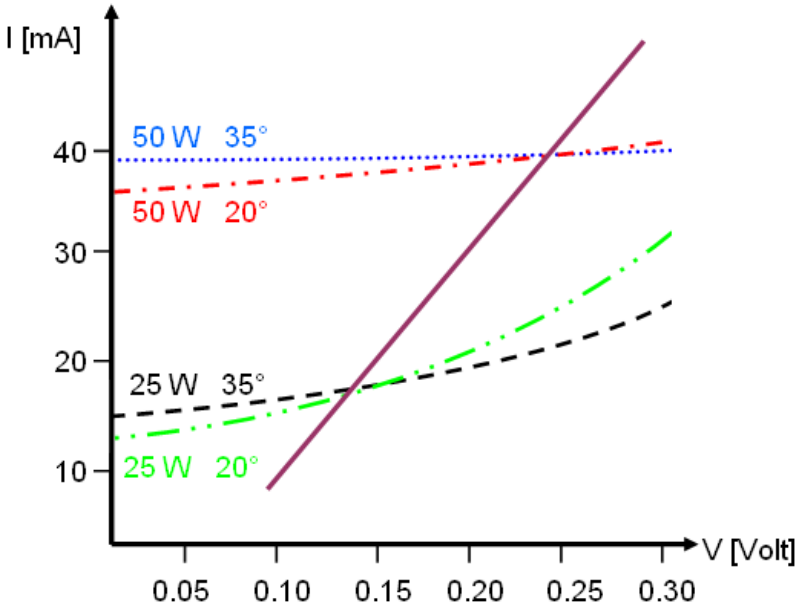

Figure 23. Experimental I-V characteristic.

For the purposes of this work, the use of pyranometer as sensing device offers better results than solarimeter one.

REFERENCES

[1] E.C. Kern Jr, E.M. Gulachenski, G. A. Kern, "Cloud effects on distributed photovoltaic generation slow transient at the gardner, Massachusetts photovoltaic experiment", IEEE Transactions On Energy Conversion, Vol. 4, No. 2, June 1989.

[2] J.H.R. Enslin, M.S.Wolf, D.B. Snyman and W. Swiegers, "Integrated photovoltaic maximum power point tracking converter", IEEE Transaction On Industrial Electronics, Vol. 44, No. 6, December 1997.

[3] R. Mukaro, X.F. Carelse, A microcontroller-based data acquisition system for solar radiation and environmental monitoring", IEEE Transaction On Instrumentation And Measurement, Vol. 48, No. 6, December 1999.

[4] E. Koutroulis, K. Kalaitzakis, N. C. Voulgaris, "Development of a microcontroller-based, photovoltaic maximum power point tracking control system", IEEE Transactions On Power Electronics, Vol. 16, No. 1, January 2001.

[5] M.A. Abella, E. Lorenzo, F. Chenlo, "Effective irradiance estimation for PV applications", 3rd World Conference On Photovoltaic Energy Conversion, May 11-18, 2003 Osaka, Japan.

[6] B. A. C. Dominguez,"Characterization of pyranometer thermal off-set and correction of historical data", Thesis submitted to the Faculty of the Virginia Polytechnic Institute and State University in partial fulfillment of the requirements for the degree of Master of Science in Mechanical Engineering, Blacksburg,Virginia, June 15, 2001

[7] D. J. Beaubien, A. Bisberg, and A. F. Beaubien, "Investigations in Pyranometer Design", Journal of Atmospheric and Oceanic Technology, Vol.15, No. 3, June, 1998.

[8] N. Femia, G. Petrone, G. Spagnuolo, M. Vitelli, Optimizing sampling rate of P&O MPPT technique", 35th Annual Ieee Power Electronics Specialists Conference, 2004, Aachen, Germany.

[9] P. Sanchis, J. López, A. Ursúa, L. Marroyo, "Electronic controlled device for the analysis and design of photovoltaic systems", IEEE Power Electronics Letters, Vol. 3, No. 2, June 2005.

[10] L. Marroyo, P. Sanchis, J. López, A. Ursúa, R. González, E. Gubía, "Equipment for the analysis of the maximum of energy of real photovoltaic systems", IEEE ISIE 2005, June 20-23, 2005, Dubrovnik, Croatia.

[11] N. Mutoh, M. Ohno, T. Inoue, A method for MPPT control while searching for parameters corresponding to weather conditions for PV generation systems", IEEE Transactions On Industrial Electronics, Vol. 53, No. 4, August 2006.

[12] A. Pandey, N. Dasgupta, A. K. Mukerjee, "A simple single-sensor MPPT solution", IEEE Transactions On Power Electronics, Vol. 22, No. 2, March 2007.

[13] Fangrui Liu, S. Duan, Fei Liu, B.Liu, Y. Kang, "A variable step size inc MPPT method for PV systems", IEEE Transactions On Industrial Electronics, Vol. 55, No. 7, July 2008.

[14] R. Gules, J. De Pellegrin Pacheco, H. Leães Hey, J. Imhoff, "A maximum power point tracking system with parallel connection for PV stand-alone applications", IEEE Transactions On Industrial Electronics, Vol. 55, No. 7, July 2008.

[15] J. Ghaisari, M. Habibi, A. Bakhshai, Member, "An MPPT controller design for photovoltaic (PV) systems based on the optimal voltage factor tracking", IEEE Canada Electrical Power Conference, 2007.

[16] C. Rodriguez, G. A. J. Amaratunga, "Analytic solution to the photovoltaic maximum power point problem", IEEE Transactions On Circuits And Systems,Vol. 54, No. 9, September 2007.

[17] G. Tina, S. Gagliano, " Probability analysis of weather data for energy assessment of hybrid solar/wind power system", 4th IASME/WSEAS International Conference on Energy, Environment, Ecosystems and Sustainable Development (EEESD'08), Algarve, Portugal, June 11-13, 2008.

[18] A. Lay-Ekuakille, G.Vendramin, A. Fedele, A.Trotta, "Photovoltaic tracking system solar radiation measurement: data validation using MPPT", 4th IASME/WSEAS International Conference on Energy, Environment, Ecosystems and Sustainable Development (EEESD'08), Algarve, Portugal, June 11-13, 2008.

[19] S. Gagliano, D. Neri, N. Pitrone, N. Savalli, G. Tina, " Design of low cost solar radiation sensing transducer for planning and monitoring of photovoltaic systems, 4th IASME/WSEAS International Conference on Energy, Environment, Ecosystems and Sustainable Development (EEESD'08), Algarve, Portugal, June 11-13, 2008.

[20] R. Attanasio, M. Cacciato, F. Gennaro, G. Scarcella, "Review on single-phase PV inverters for grid-connected applications", 4th IASME/WSEAS International Conference on Energy, Environment, Ecosystems and Sustainable Development (EEESD'08), Algarve, Portugal, June 11-13, 2008.

[21] G. Tina, G. Gozzo, P.Arena, L. Patanè, S. De Fiore, "Design of a robot photovoltaic power supply system", 4th IASME/WSEAS International Conference on Energy, Environment, Ecosystems and Sustainable Development (EEESD'08), Algarve, Portugal, June 11-13, 2008.

[22] L. Corradini, "Fundamentals of automatic control", Pitagora Editrice, Bologna, Italy, 2002.